Preprints of the 18th IFAC World Congress
Milano (Italy) August 28 - September 2, 2011

# Landing gear suspension control through adaptive backstepping techniques with $H_\infty$ performance

**Mauricio Zapateiro** * **Francesc Pozo** * **Josep M. Rossell** **
**Hamid Reza Karimi** *** **Ningsu Luo** ****

* *Department of Applied Mathematics III, Universitat Politècnica de Catalunya–BarcelonaTECH, Comte d'Urgell 187, 08036 Barcelona, Spain.*
** *Department of Applied Mathematics III, Universitat Politècnica de Catalunya–BarcelonaTECH, Av. Bases de Manresa 61-73, 08240 Manresa, Spain*
*** *Department of Engineering, Faculty of Engineering and Science, University of Agder, N-4898 Grimstad, Norway.*
**** *Institute of Informatics and Applications, University of Girona, Campus de Montilivi, Ed.P4, 17071 Girona, Spain.*

**Abstract:**
Landing gear suspension systems fulfill the tasks of absorbing the vertical energy of the touch-down as well as providing passenger and crew comfort with a smooth ground ride before take-off and after landing. They are also designed to have optimal performance in the case of a hard landing. In general, the tasks of aircraft landing gears are complex and sometimes lead to a number of contradictory requirements. Although there are existing modifications of aircraft shock absorbers to reduce the problem, the basic design conflict between the requirements for landing and for rolling cannot be fully overcome by a passive suspension layout. Active and semiactive suspension techniques are a solution to this problem and are capable of reducing fuselage vibrations effectively. In order to get satisfactory damping performance with active and semiactive devices, appropriate control laws must be employed. In this paper, we study the use of an adaptive backstepping control with $H_\infty$ performance to cope with disturbances, uncertainties and nonlinearities, typical of suspension systems and damping devices. A comparison between active and semiactive strategies is provided through the analysis of simulation results.

## 1. INTRODUCTION

Suspension systems are one of the most critical parts of transportation vehicles. A good suspension system should be able to provide safety to both passengers and loads and protect the vehicle from damage caused by the unevenness of the roads. In aircrafts, the landing gears fulfill these tasks. Not only are they designed to provide comfort during taxiing but absorb the energy during touch down. Landing gears mainly consist of a strut attached to the aircraft fuselage. The strut is coupled to the ground via one or more wheels with flexible tyres mounted on an axle [1]. Landing gears are normally equipped with passive damping devices that absorb the energy. However, there may be cases when the impact is large because the damper cannot be tuned for every single runway characteristics. This is why active and semiactive absorbers are currently being studied and experimented to overcome the adaptability problem [2]. Compared with passive dampers, active and semiactive devices can be tuned due to their flexible structure. One of the drawbacks of active dampers is that they may become unstable if the controller fails. On the contrary, semiactive devices are inherently stable because they cannot inject energy. Thus, the latter acts as pure passive dampers in case of control failure [3].

In recent years, there has been an increasing interest in the control of suspension systems using both active and semiactive dampers. As such, different control techniques have been applied. For instance, in [4], it is proposed a semiactive controller based on a hybrid approach that combines a non-linear PID term based on the expression of the shock absorber viscous force contribution; in [3], a kind of Nonlinear Model Predictive Control algorithm (NMPC) for semiactive landing gears is developed using Genetic Algorithms (GA) as the optimization technique and chooses damping performance of landing gear at touch down to be the optimization object; in [5], a semiactive backstepping controller is proposed as a means to control a magnetorheological damper for suspension systems; in [6] a fuzzy adaptive output feedback controller to control landing gear shimmy through active damping is proposed; in [7], a hybrid control of active suspension systems for quarter-car models with two-degree-of-freedom is implemented by controlling the linear part with $H_\infty$ techniques and the nonlinear part with and adaptive controller based

on backstepping. In this paper, as an extension to previous works, an adaptive backstepping control with $H_\infty$ techniques is presented. To the best of the authors' knowledge, this idea has not been deeply developed, being the work by Li and Liu [9] one example on this topic. Their method integrates the adaptive dynamics surface control and $H_\infty$ control techniques guaranteeing that the output tracking error satisfies the $H_\infty$ tracking performance. The contribution of our paper is two-fold: first, this paper extends previous works on backstepping problem; second, by utilizing an adaptive technique, using a Lyapunov function and a suitable change of backstepping variables, we derive the explicit expression of the controllers to satisfy both asymptotic stability and an $H_\infty$ performance for the controlled system.

This paper is organized as follows. In Section 2, a detailed description of the model of the suspension system of the landing gear is presented. Section 3 explains the target problem and the objective of the control to be designed. Then, the details on the control formulation are outlined in Section 4. The controller performance is analyzed in Section 5. The conclusions are outlined in Section 6.

## 2. SYSTEM DESCRIPTION

The aircraft landing gear can be modeled as a quarter car model as shown in Figure 1. It is composed of two subsystems: the tyre subsystem and the suspension subsystem. The tyre subsystem is represented by the wheel mass $m_u$ while the suspension subsystem consists of a sprung mass, $m_s$, that resembles the aircraft mass. The compressibility of wheel pneumatic is $k_t$, while $c_s$ and $k_s$ are the damping and stiffness of the uncontrolled suspension system. The following state variables are used to model the system: $x_1$ is the tyre deflection, $x_2$ is the unsprung mass velocity, $x_3$ is the suspension deflection and $x_4$ is the sprung mass velocity. Thus, the state space representation of the system of Figure 1 is:

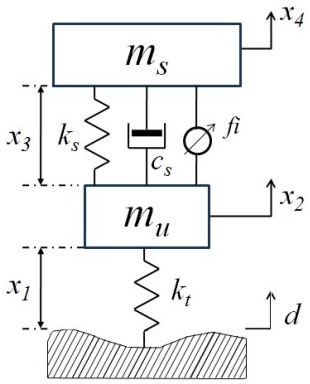


Fig. 1. Landing gear model

- Tyre subsystem:

$$\begin{aligned} \dot{x}_1 &= x_2 - d \\ \dot{x}_2 &= -\tfrac{k_t}{m_u} x_1 + \rho u \end{aligned} \tag{1}$$

- Suspension subsystem:

$$\begin{aligned} \dot{x}_3 &= -x_2 + x_4 \\ \dot{x}_4 &= -u \end{aligned} \tag{2}$$

where $\rho = m_s/m_u$, $d$ is the velocity of the input disturbance and $u$ is the acceleration input due to the damping subsystem. The input $u$ is given by:

$$u = m_s^{-1}(k_s x_3 + c_s(x_4 - x_2) + f_i) \tag{3}$$

where $f_i$ is the damping force generated by the active or semiactive device.

## 3. PROBLEM STATEMENT

In this section we present the details of the active and semiactive controller for the aircraft landing gear. The objective is to design an adaptive backstepping controller to regulate the suspension deflection of the landing gear with the aid of a damper, either active or semiactive, thus providing safety and comfort while the aircraft is taxiing on the runways. The adaptive backstepping controller will be designed in such a way that, for a given $\gamma > 0$, the state-dependent error variables $e_1$ and $e_2$ (to be defined later) accomplish the following $H_\infty$ performance if $J_\infty < 0$:

$$J_\infty = \int_0^\infty (\mathbf{e}^T \mathbf{R} \mathbf{e} - \gamma^2 \mathbf{w}^T \mathbf{w}) dt \tag{4}$$

where $\mathbf{e} = (e_1, e_2)^{\mathrm{T}}$ is a vector of controlled signals, $\mathbf{R} = \mathrm{diag}\{r_1, r_2\}$ is a positive definite matrix and $\mathbf{w}$ is the vector of incoming disturbances.

In order to formulate the adaptive backstepping controller, the state space model of Eqs. (1) - (2) must be first written in strict feedback form [8]. Therefore, the following coordinate transformation is performed [10]:

$$\begin{aligned} z_1 &= x_1 + \rho(\rho+1)^{-1} x_3 \\ z_2 &= (\rho+1)^{-1} x_2 + \rho(\rho+1)^{-1} x_4 \\ z_3 &= x_3 \\ z_4 &= -x_2 + x_4 \end{aligned} \tag{5}$$

The system, represented in the new coordinates, is given by:

- tyre subsystem:

$$\begin{aligned} \dot{z}_1 &= z_2 - d \\ \dot{z}_2 &= -k_t[m_u(\rho+1)]^{-1} z_1 + \rho k_t [m_u(\rho+1)^2]^{-1} z_3 \end{aligned} \tag{6}$$

- Suspension subsystem:

$$\begin{aligned} \dot{z}_3 &= z_4 \\ \dot{z}_4 &= k_t m_u^{-1} z_1 - k_t \rho [m_u(\rho+1)]^{-1} z_3 - (\rho+1) u \end{aligned} \tag{7}$$

Substitution of the expression for $u$ (Eq. 3) in Eq. 7 yields:

$$\begin{aligned} \dot{z}_3 =& z_4 \\ \dot{z}_4 =& k_t m_u^{-1} z_1 - k_t \rho [m_u(\rho+1)]^{-1} z_3 \\ & - (\rho+1) m_s^{-1} [k_s x_3 + c_s(x_4 - x_2) + f_i] \\ =& d_i - a_k z_3 - a_c z_4 - a_f f_i \end{aligned} \tag{8}$$

where $a_k = [k_t \rho(\rho+1)^{-1} + (\rho+1) k_s] m_u^{-1}$, $a_c = (\rho+1) m_s^{-1} c_s$ and $a_f = (\rho+1) m_s^{-1}$; $d_i = k_t m_s^{-1} z_1$ reflects the fact that the disturbance enters to the suspension subsystem through the tyre subsystem. $a_k$ and $a_c$ are uncertain constant parameters whose estimated values are $\hat{a}_k$ and $\hat{a}_c$, respectively. Thus, the errors between the estimates and the actual values are given by:

$$\begin{aligned} \tilde{a}_k &= a_k - \hat{a}_k \\ \tilde{a}_c &= a_c - \hat{a}_c \end{aligned} \tag{9}$$

Let $a_1 = k_t[m_s(\rho+1)]^{-1}$, $a_2 = \rho k_t[m_s(\rho+1)^2]^{-1}$ and $a_m = k_t m_s^{-1}$. From Eqs. (6) - (7), it can be shown that the transfer functions from $d(t)$ and $f_i(t)$ to $z_1(t)$ are:

$$\frac{Z_1(s)}{D(s)} = \frac{-s(s^2 + a_c s + a_k)}{s^4 + a_c s^3 + (a_1 + a_k)s^2 + a_1 a_c s + a_1 a_k - a_m a_2} \tag{10}$$

$$\frac{Z_1(s)}{F_i(s)} = \frac{-a_2 a_f}{s^4 + a_c s^3 + (a_1 + a_k)s^2 + a_1 a_c s + a_1 a_k - a_m a_2} \tag{11}$$

If the poles of the transfer functions of Eqs. (10) and (11) are in the left side of the $s$ plane, then we can guarantee the bounded input - bounded output (BIBO) stability of $Z_1(s)$ for any bounded input $D(S)$ and $F_i(s)$. Thus, the disturbance input $d_i(t)$ in Eq. (8) is also bounded. This boundedness condition will be used later in the controller formulation.

Finally, since $d_i$ is the only disturbance input to the suspension subsystem, the vector $\mathbf{w}$ of the $H_\infty$ performance objective as given in Eq. (4) becomes:

$$J_\infty = \int_0^\infty (\mathbf{e}^T \mathbf{R} \mathbf{e} - \gamma^2 d_i^2) dt \tag{12}$$

## 4. CONTROLLER FORMULATION

In order to begin with the adaptive backstepping design, we firstly define the following error variable and its derivative:

$$e_1 = z_3 \tag{13}$$

$$\dot{e}_1 = \dot{z}_3 = z_4 \tag{14}$$

Now, the following Lyapunov function candidate is chosen:

$$V_1 = \frac{1}{2} e_1^2 \tag{15}$$

whose first-order derivative is:

$$\dot{V}_1 = e_1 \dot{e}_1 = e_1 z_4 \tag{16}$$

Equation (14) can be stabilized with the following virtual control input:

$$z_{4d} = -r_1 e_1 \tag{17}$$

$$\dot{z}_{4d} = -r_1 \dot{e}_1 = -r_1 z_4 \tag{18}$$

where $r_1 > 0$. Now define a second error variable and its derivative:

$$e_2 = z_4 - z_{4d} \tag{19}$$

$$\dot{e}_2 = \dot{z}_4 - \dot{z}_{4d} \tag{20}$$

Therefore,

$$\dot{V}_1 = e_1 z_4 = e_1(e_2 - r_1 z_4) = e_1 e_2 - r_1 e_1 z_4 \tag{21}$$

On the other hand, the derivatives of the errors of the uncertain parameter estimations are given by:

$$\dot{\tilde{a}}_k = -\dot{\hat{a}}_k \tag{22}$$

$$\dot{\tilde{a}}_c = -\dot{\hat{a}}_c \tag{23}$$

Now, an augmented Lyapunov function candidate is chosen:

$$V = V_1 + \frac{1}{2} e_2^2 + \frac{1}{2 r_k} \tilde{a}_k^2 + \frac{1}{2 r_c} \tilde{a}_c^2 \tag{24}$$

Thus, by using Eqs. (19) - (23) and the fact that $a_k = \tilde{a}_k + \hat{a}_k$ and $a_c = \tilde{a}_c + \hat{a}_c$, the derivative of $V$ yields:

$$\begin{aligned}
\dot{V} =& e_1 \dot{e}_1 + e_2 \dot{e}_2 + r_k^{-1} \tilde{a}_k \dot{\tilde{a}}_k + r_c^{-1} \tilde{a}_c \dot{\tilde{a}}_c \\
=& e_1 e_2 - r_1 e_1^2 + e_2 d_i - a_k z_3 e_2 - a_c z_4 e_2 - a_f f_i e_2 \\
& - r_1 z_4 e_2 - r_k^{-1} \tilde{a}_k \dot{\tilde{a}}_k - r_c^{-1} \tilde{a}_c \dot{a}_c \\
=& e_1 e_2 - r_1 e_1^2 + e_2 d_i - a_f f_i e_2 - r_1 z_4 e_2 - r_k^{-1} \tilde{a}_k \dot{\hat{a}}_k \\
& - (\tilde{a}_k + \hat{a}_k) z_3 e_2 - (\tilde{a}_c + \hat{a}_c) z_4 e_2 - r_c^{-1} \tilde{a}_c \dot{\hat{a}}_c \\
=& e_1 e_2 - r_1 e_1^2 + e_2 d_i - \tilde{a}_k (z_3 e_3 + r_k^{-1} \dot{\hat{a}}_k) - \hat{a}_k z_3 e_2 \\
& - \tilde{a}_c (z_4 e_2 + r_c^{-1} \dot{\hat{a}}_c) - \hat{a}_c z_4 e_2 + a_f f_i e_2 - r_1 z_4 e_2
\end{aligned} \tag{25}$$

Now consider the following adaptation laws:

$$z_3 e_1 + r_k^{-1} \dot{\hat{a}}_k = 0 \tag{26}$$

$$z_4 e_2 + r_c^{-1} \dot{\hat{a}}_c = 0 \tag{27}$$

Substitution of Eqs. (26) and (27) into Eq. (25) yields:

$$\dot{V} = -r_1 e_1^2 + e_2 d_i + e_2(e_1 - \hat{a}_k z_3 - \hat{a}_c z_4 + a_f f_i - r_1 z_4) \tag{28}$$

By choosing the following control law:

$$f_i = -a_f^{-1}(e_1 - \hat{a}_k z_3 - \hat{a}_c z_4 - r_1 z_4 + r_2 e_2 + e_2 (2\gamma)^{-2}) \tag{29}$$

with $\gamma > 0$ and $r_2 > 0$, we get:

$$\begin{aligned}
\dot{V} =& - r_1 e_1^2 + e_2 d_i - r_2 e_2^2 - e_2 (2\gamma)^{-2} \\
=& - r_1 e_1^2 + e_2 d_i - r_2 e_2^2 - e_2 (2\gamma)^{-2} \\
& + \gamma^2 d_i^2 - \gamma^2 d_i^2 \\
=& - r_1 e_1^2 - r_2 e_2^2 + \gamma^2 d_i^2 - (\gamma d_i - e_2 (2\gamma)^{-2})^2 \\
\dot{V} \leq& - r_1 e_1^2 - r_2 e_2^2 + \gamma^2 d_i^2
\end{aligned} \tag{30}$$

The objective of guaranteeing global boundedness of trajectories is equivalently expressed as rendering $\dot{V}$ negative outside a compact region. As stated earlier in Section 3, the disturbance input $d_i$ is bounded as long as the poles of the transfer functions (10) and (11) are in the left side of the $s$ plane. When this is the case, the boundedness of the input disturbance $d_i$ guarantees the existence of a small compact region $D \subset \mathbb{R}^2$ (depending on $\gamma$ and $d_i$ itself) such that $\dot{V}$ is negative outside this set. More precisely, when $r_1 e_1^2 + r_2 e_2^2 < \gamma^2 d_i^2$, $\dot{V}$ is positive and then the error variables are increasing values. Finally, when the expression $r_1 e_1^2 + r_2 e_2^2$ is greater than $\gamma^2 d_i^2$, $\dot{V}$ is then negative. This implies that all the closed-loop trajectories have to remain bounded, as we wanted to show. Now, under zero initial conditions, we can write:

$$\begin{aligned}
\int_0^\infty \dot{V}\, dt \leq& - \int_0^\infty r_1 e_1^2\, dt - \int_0^\infty r_2 e_2^2\, dt \\
& + \int_0^\infty \gamma^2 d_i^2\, dt \\
V|_{t=\infty} - V|_{t=0} \leq& - \int_0^\infty \mathbf{e}^T \mathbf{R} \mathbf{e}\, dt + \gamma^2 \int_0^\infty d_i^2\, dt \\
J_\infty =& \int_0^\infty (\mathbf{e}^T \mathbf{R} \mathbf{e} - \gamma^2 d_i^2)\, dt \leq -V|_{t=\infty} \leq 0
\end{aligned} \tag{31}$$

Thus, the adaptive backstepping controller satisfies the $H_\infty$ performance and the asymptotic stability of the system is guaranteed.

The control force given by Eq. (29) can be used to drive an actively controlled damper. However, the fact that semiactive devices cannot inject energy into a system, makes necessary the modification of this control law in order to implement it with a semiactive damper; that is, semiactive dampers cannot apply force to the system, only absorb. There are different ways to perform this [17, 14]. In this work, we will use the algorithm by [11], which computes the control signal based on the force required by the control law and the force that the damper is currently generating:

$$v = V_{max} \cdot H\left\{(f_i - f_m)\, f_m\right\} \tag{32}$$

where $v$ is the damper input control signal, $f_i$ is the active control input, $f_m$ is the current damping force, $H\{\cdot\}$ is the Heaviside function and $V_{max}$ is the highest value of the damper input control signal. The control signal $v$ can be a voltage or current signal that drives the mechanism of the semiactive damper to provide the required damping force.

Since the controller is derived using the backstepping technique, nonlinearities and uncertainties can be accounted for by including them in the development of the control law as done in [17].

## 5. NUMERICAL RESULTS

The controllers of Eqs. (29) and (32) were implemented in MATLAB/Simulink in order to evaluate their performance. The landing gear model (Eqs. 1 - 2) was implemented with the following values: $m_s$=11739 kg, $m_u$=300 kg, $k_s$=252000 N/m, $c_s$=10000 N-s/m and $k_t$=300000 N/m. With these values, the poles of the transfer functions of Eqs. (10) and (11) are $-0.34\times10^{-3}\pm j0.78$ and $-17.09\pm j24.38$ and thus, the disturbance input $d_i$ is bounded. In order to compare the active and the semiactive controllers, we assume that:

- The dynamics of the active damper is given by the first order filter
$$\frac{F_f(s)}{F_i(s)} = \frac{60}{s+60} \tag{33}$$
where $F_f(s)$ is the Laplace transform of the output of the active damper and $F_i(s)$ is also the Laplace transform of the active control force.
- The dynamics of the semiactive damper is given by the Bouc-Wen model of a magnetorheological damper [12, 16]:
$$\begin{aligned} f_m =& (c_{02}(x_4 - x_2) + k_{02}x_3 + \delta_{02}\xi)v \\ &+ (c_{01}(x_4 - x_2) + k_{01}x_3 + \delta_{01}\xi) \end{aligned} \tag{34}$$
$$\begin{aligned} \dot{\xi} =& -\kappa|x_4 - x_2|\xi|\xi|^{n-1} - \beta(x_4 - x_2)|\xi|^n \\ &+ A(x_4 - x_2) \end{aligned} \tag{35}$$
where $c_{01} + c_{02}v$ and $k_0 = k_{01} + k_{02}v$ are the damping and stiffness of the damper, which depend on a voltage control input ($v$), $\xi$ is an evolutionary variable that accounts for the hysteretic dynamics of the device and $A$, $\beta$, $\kappa$ and $n$ are parameters that control the shape of the hysteresis loop.

The value of the Bouc-Wen model parameters are [13]: $\alpha$=33.27 N/m, $\alpha$=182.65 N/m-V, $c_{01}$=754.41 Ns/m, $c_{02}$=712.73 Ns/m-V, $k_{01}$=1137.57 N/m, $k_{02}$=1443.50 N/m-V, $\kappa$=4209.8 m$^{-2}$, $\beta$=4205.2 m$^{-2}$, $A$=10246 and $n$=2. Since this is a mid scale damper, able to generate approximately 3000 N at low velocities, the damping force is scaled by a factor of 10 in order to make it suitable for this landing gear system. The adaptive backstepping controller is implemented with $r_1$=1, $r_2$=100, $r_c$=1, $r_k$=5 and $\gamma$=0.2. The performance indices $J_1$ – $J_8$ of Table 1 were used to numerically evaluate the controller performances. Indices $J_1$ – $J_6$ show the ratio between the peak and root mean square (RMS) values of of the system response (suspension deflection, sprung mass velocity and sprung mass acceleration) in the controlled case ('active' and 'semiactive') with respect to the uncontrolled case ('unc', in the figures). $J_7$ is the RMS value of the control effort and $J_8$ is a measure of the $H_\infty$ performance.

| **Index** | **Definition, [Units]** |
|---|---|
| $J_1 = \frac{max\|x_3(t)\|_{cont}}{max\|x_3(t)\|_{unc}}$ | Pk. susp. defl. ratio, [m]. |
| $J_2 = \frac{max\|x_4(t)\|_{cont}}{max\|x_4(t)\|_{unc}}$ | Pk. sprung mass vel. ratio, [m/s]. |
| $J_3 = \frac{max\|\dot{x}_4(t)\|_{cont}}{max\|\dot{x}_4(t)\|_{unc}}$ | Pk. spr. mass accel. ratio, [m/s$^2$]. |
| $J_4 = \frac{RMS(x_3(t))_{cont}}{RMS(x_3(t))_{unc}}$ | Susp. defl. RMS ratio, [adim.]. |
| $J_5 = \frac{RMS(x_4(t))_{cont}}{RMS(x_4(t))_{unc}}$ | Spg. mass vel. RMS ratio, [adim.]. |
| $J_6 = \frac{RMS(\dot{x}_4(t))_{cont}}{RMS(\dot{x}_4(t))_{unc}}$ | Spg. mass accel. RMS ratio, [ad.]. |
| $J_7 = RMS(f_i)$ | Control effort RMS, [N]. |
| $J_8 = \frac{\sqrt{\|\|[r_1^{1/2}e_1\ r_2^{1/2}e_2]^T\|\|}}{\sqrt{\|\|d_i\|\|}}$ | $H_\infty$ performance, [adim.]. |

Table 1. Performance indices.

The system is first excited with the random input of Figure 2. In Figure 3 we can observe the system response to this input, in particular, the suspension deflection and the sprung mass velocities and accelerations obtained with the active and the semiactive dampers. It can be noted that both dampers have a similar performance and also that they get to significantly reduce the sprung mass velocity. In Figure 4, a comparison between the control effort of the active and the semiactve dampers is depicted. On the other hand, the tyre-unsprung mass subsystem through which the disturbance enters the sprung mass, responded satisfactorily during the simulations as can be observed in Figure 5. In spite of the fact that, for design purposes, this subsystem was not explicitly considered in the formulation of the control law, the effect of the controllers on it were the reduction of the tyre deflection and the unsprung mass velocity.

The performance indices of these controllers appear in Table 2. This table shows a reduction in the suspension deflection peaks and RMS values. At the beginning of the control action, the peak acceleration is almost the same in all controlled and uncontrolled cases, but the controllers attempt to reduce it afterwards, as index $J_6$ shows. Index $J_7$ shows that the control effort achieved by the semiactive controller is less than that of the active controller, while index $J_8$ shows that the value of the $H_\infty$ performance of both controllers is less than that of the prescribed $\gamma$.

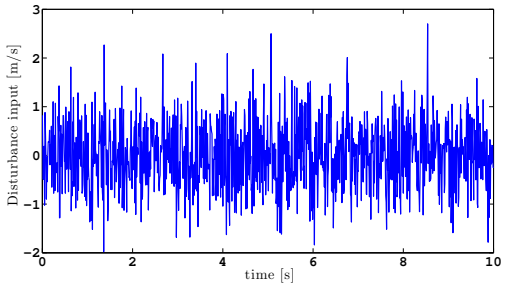


Fig. 2. Random disturbance input.

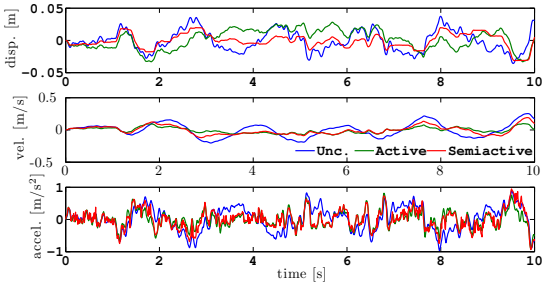


Fig. 3. System response to the random disturbance input.

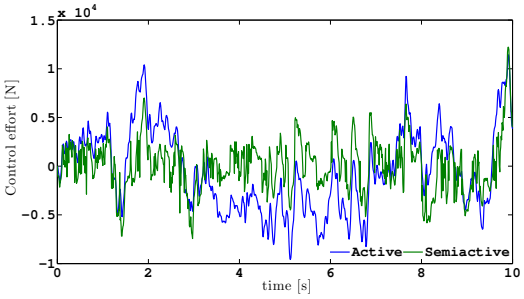


Fig. 4. Control effort during the random disturbance input.

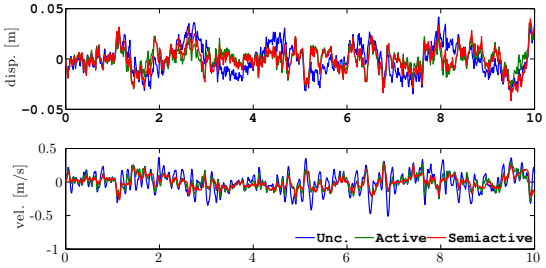


Fig. 5. tyre deflection and unsprung mass velocity.

| Index | Active control | Semiactive control |
|---|---|---|
| $J_1$ | 0.8861 | 0.8365 |
| $J_2$ | 0.3879 | 0.7558 |
| $J_3$ | 0.9669 | 0.9851 |
| $J_4$ | 0.9578 | 0.6897 |
| $J_5$ | 0.4164 | 0.6179 |
| $J_6$ | 0.6755 | 0.8151 |
| $J_7$ | 4232.3 | 2718.2 |
| $J_8$ | 0.0525 | 0.0446 |

Table 2. Performance indices for the random input case.

The next simulation was performed with a bump-like disturbance input, shown in Figure 6 and the system response is shown in Figure 7. In this figure, it is readily observed the reduction in suspension deflection and sprung mass velocities and accelerations achieved by both controllers. The control effort of both dampers can be seen in Figure 8. The tyre deflection and the unsprung mass velocity are shown in Figure 9, where it can observed a significant reduction with respect to the uncontrolled cases.

Despite the peak velocities and accelerations are slightly higher than in the uncontrolled cases, this occurs only at the beginning of the excitation and their values are significantly reduced after this. These facts are also reflected in Table 3, where it can also be noted that the control effort of the semiactive controller is less than that of the active one. From these simulations, it can be seen that in spite of the fact that active and semiactive control performances are similar, the difference relies in favor of the semiactive controller.

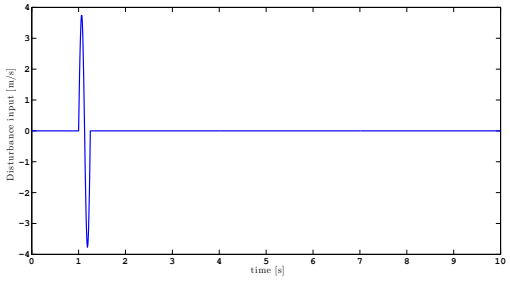


Fig. 6. Bump-like disturbance input.

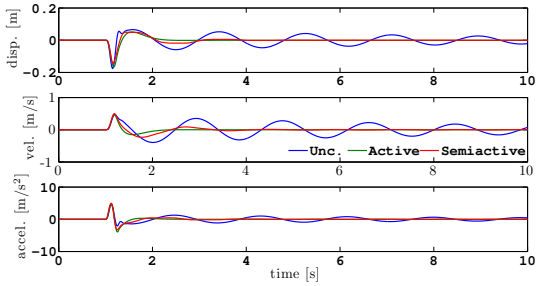


Fig. 7. System response to the bump-like disturbance input.

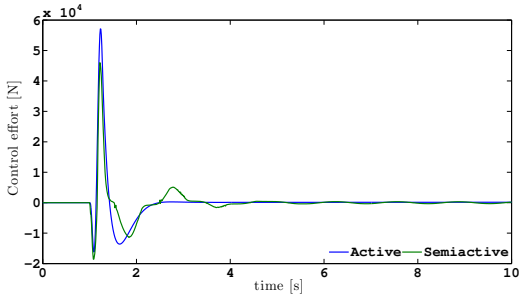


Fig. 8. Control effort during the bump-like disturbance input.

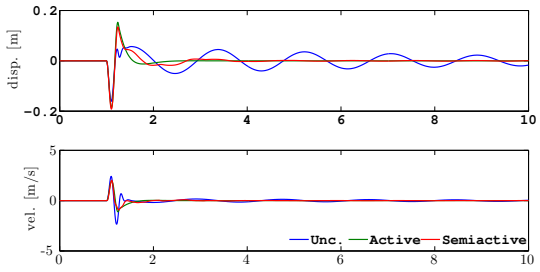


Fig. 9. tyre deflection and unsprung mass velocity.

| Index | Active control | Semiactive control |
|---|---|---|
| $J_1$ | 0.9399 | 0.8220 |
| $J_2$ | 0.9912 | 1.0661 |
| $J_3$ | 1.0240 | 1.0779 |
| $J_4$ | 0.6001 | 0.5655 |
| $J_5$ | 0.3123 | 0.4129 |
| $J_6$ | 0.7828 | 0.7929 |
| $J_7$ | 6402.9 | 4917.0 |
| $J_8$ | 0.1913 | 0.1835 |

Table 3. Performance indices for the bump-like input case.

## 6. CONCLUSIONS

In this paper we have explored the design of an adaptive backstepping controller for the suspension system of a landing gear. The controller was designed in such a way the tracking errors achieved an $H_\infty$ performance. This class of control allows to account for uncertainties, nonlinearities and disturbances in a systematic way. Two controllers were formulated: an active and a semiactive. This allowed to make a comparison between two usual schemes in suspension systems which consist of adding active or semiactive dampers to improve the performance of the pure passive damping system. As a result, the vibrations in the sprung mass of the system were significantly reduced in both active and semiactive cases. Despite the performance of the active and semiactive controllers were similar, it could be noted that the semiactive controller required of less control effort to achieve the objectives.

## 7. ACKNOWLEDGMENTS

This work has been partially funded by the European Union (European Regional Development Fund) and the Ministry of Science and Innovation of Spain through the coordinated research projects DPI2008-06699-C02 and DPI2008-06463-C02-01, and by the Government of Catalonia (Spain) through SGR523 and SGR2009-1228. M. Zapateiro is also supported by the 'Juan de la Cierva' Fellowship from the Ministry of Science and Innovation.

## REFERENCES

[1] P. Thota, B. Krauskopf, M. Lowenberg, "Shimmy in a nonlinear model of an aircraft nose landing gear with non-zero rake angle", EUROMECH Nonlinear Dynamics Conference, St. Petersburg, Russia, 2008.

[2] H. Wang, J.T. Xing, W.G. Price, W. Li, "An investigation of an active landing gear system to reduce aircraft vibrations caused by landing impacts and runway excitations", Journal of Sound and Vibration, Vol. 317, pp. 50-66, 2008.

[3] D.S. Wu, H.B. Gu, H. Liu, "GA-based model predictive control of semi-active landing gear", Chinese Journal of Automatics, Vol. 20, pp. 47-54, 2007.

[4] G.L. Ghiringhelli, S. Gualdi, "Evaluation of a landing gear semi-active control system for complete aircraft landing", Aerotecnica Missili e Spazio, Vol. 83, 21-31, 2004.

[5] M. Zapateiro, N. Luo, H.R. Karimi, J. Vehí, "Vibration control of a class of semiactive suspension system using neural network and backstepping techniques", Mechanical Systems and Signal Processing, Vol. 23, 1946-1953, 2009.

[6] G. Pouly, T.H. Huynh, J.P. Lauffenburger, M. Basset, "Active shimmy damping using Fuzzy Adaptive output feedback control", $10^{th}$ International Conference on Control, Automation, Robotics and Vision, Hanoi, Vietnam, 2008.

[7] T.T. Nguyen, T.H. Bui, T.P. Tran, S.B. Kim, "A hybrid control of active suspension system using $H_\infty$ and nonlinear adaptive controls", IEEE Int. Symp. on Ind. Elect., Pusan, Korea, 2001.

[8] M. Krstic, I. Kanellakopoulos, O. Kokotovic, " Nonlinear and Adaptive Control Design", John Wiley and Sons, Inc., 1995.

[9] W. Li and X. Liu, "Robust adaptive tracking control of uncertain electrostatic micro-actuators with H-infinity performance", *Mechatronics*, vol. 19, pp. 591-597, 2009.

[10] N. Karlsson, A. Teel, D. Hrovat, "A backstepping approach to control of active suspensions", Proceedings of the 40th IEEE Conference on Decision and Control, Orlando, Florida, USA, 2001.

[11] S.J. Dyke, B.F. Spencer, M.K. Sain, and J.D. Carlson, "Modeling and control of magnetorheological dampers for seismic response reduction" *Smart Materials and Structures*, vol. 5, pp. 565-575, 1996.

[12] B.F. Spencer, Jr., S.J. Dyke, M. Sain, J.D. Carlson, "Phenomenological model of a magnetorheological damper", ASCE Journal of Engineering Mechanics, Vol. 123, pp. 230-238, 1997.

[13] J. Carrion, B.F. Spencer, Jr., "Model-based strategies for real-time hybrid testing", Technical Report, University of Illinois at Urbana-Champaign, 2007.

[14] A. Bahar, F. Pozo, L. Acho, J. Rodellar, A. Barbat, "Hierarchical semi-active control of base-isolated structures using a new inverse model of magnetorheological dampers", Computers and Structures, Vol. 88, pp. 483-496, 2010.

[15] A. Bahar, F. Pozo, L. Acho, J. Rodellar, A. Barbat, "Parameter identification of large-scale magnetorheological dampers in a benchmark building", Computers and Structures, Vol. 88, pp. 198-206, 2009.

[16] F. Pozo, L. Acho, A. Rodríguez, G. Pujol, "Nonlinear modeling of hysteretic systems with double hysteretic loops using position and acceleration information", Nonlinear Dynamics, Vol. 57, pp. 1-12, 2009.

[17] M. Zapateiro, H.R. Karimi, N. Luo, B.F. Spencer, Jr., "Real-time hybrid testing of semiactive control strategies for vibration reduction in a structure with MR damper", Struct. Cont. and Health Monit., Vol. 17, 427-451, 2009.